The development of a conical composite energy absorber for use in the attenuation of crash/impact loads

Authors: Justin D. Littell

ABSTRACT

A design for a novel light-weight conical shaped energy absorbing (EA) composite subfloor structure is proposed. This composite EA is fabricated using repeated alternating patterns of a conical geometry to form long beam structures which can be implemented as aircraft subfloor keel beams or frame sections. The geometrical features of this conical design, along with the hybrid composite materials used in the manufacturing process give a strength tailored to achieve a constant 25-40 g sustained crush load, small peak crush loads and long stroke limits. This report will discuss the geometrical design and fabrication methods, along with results from static and dynamic crush testing of 12-in. long subcomponents.

Justin D. Littell, NASA Langley Research Center. 14 W. Bush Rd, Hampton VA 23681, MS 495.
Justin.D.Littell@nasa.gov, (757) 864-5095

BACKGROUND

In 2013, a full scale crash test of a CH-46 helicopter airframe was conducted at the NASA Langley Research Center's (LaRC) Landing and Impact Research Facility under the Rotary Wing Crashworthiness Program. The Transport Rotorcraft Airframe Crash Tested (TRACT) crash test was conducted in collaboration with the LaRC, ARMY, NAVY, FAA and industry partners with goals of evaluating various seat designs, Anthropomorphic Test Device (ATD, a.k.a. crash test dummy) responses, restraints, and novel data acquisition techniques [1]. Additionally, one of the goals of the crash test was to generate baseline test data for comparison with data from a second full scale crash test, TRACT 2, which will be conducted in late 2014. The baseline data, consisting of airframe accelerations, occupant loads, and airframe deformation were all acquired during the TRACT 1 test. While the TRACT 2 test will have similar seat, occupant and restraint experiments, one of the major goals of the test is to evaluate novel composite energy absorbing subfloor designs for improved crashworthiness of the airframe structure. The goal is to generate data on these composite energy absorbers, which could be eventually incorporated or retrofitted into current fleets of aircraft. However, in order to be considered for inclusion into the TRACT 2 test, the energy absorbing designs must excel in two major criteria. First, they must limit the load to tolerable levels for human occupants by providing equivalent or lower load levels than their metallic counterparts, and, second, they must also still be viable for use as a structural airframe member by providing airworthy structural rigidity.

This report will discuss one candidate under consideration for inclusion into the TRACT 2 test: a novel conical sinusoid, or a "conusoidal" composite energy absorbing (EA) concept. The following sections will present the background concept, material evaluation and selection, along with the component fabrication process of the conusoidal concept. Finally, results from conusoidal subcomponent tests will be presented and further compared to a more conventional EA design.

DEVELOPMENT AND FABRICATION

The conusoidal geometry is based on right-side-up and up-side down half-cones placed in an alternating and repeating pattern. This geometry combines a simple cone design which has been extensively studied in literature [2-5] with a sinusoidal beam geometry to create a structure which utilizes the advantages of both designs. The first major advantage of the conusoidal design is it provides crush trigger mechanisms due to dissimilar conical radii dimensions on the crash front.

This is consistent with many EA designs which contain trigger mechanisms to limit the peak crush load and achieve acceptable crush initiation behavior. Second, because the conical walls are formed at an inward angle relative to the geometric centerline of each cone, the crushing is self-stabilizing. Finally, as Figure 1 (side view) shows, the dissimilar radii create an inherent forward leaning angle, which offers advantages when examining loading conditions with a multi-axial component of loading. Rotorcraft impact scenarios in many cases involve both vertical and forward velocities. Figure 1 shows a rendering of the conusoidal design.

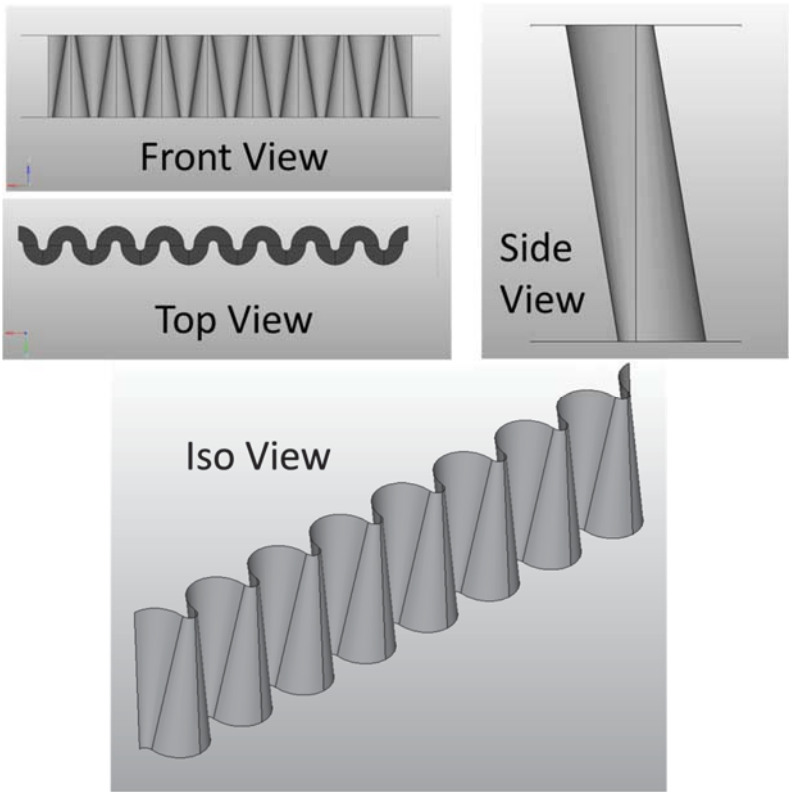

Figure 1. Conusoidal Concept

A literature survey was completed to investigate both crushable beam designs along with results arising from conical crushing. The final configurations were dimensionally similar to other sinusoidal designs which have been reported [6-9]. However, the specimen geometry and general dimensions were mainly chosen based on an existing sinusoidal mold present at LaRC previously built for an aircraft EA keel beam. Also, by designing conusoids dimensionally similar to the existing sinusoidal hardware, direct comparisons between the conusoid and the sinusoid can be made. Thus, using the existing sinusoidal mold as a guide, longitudinal midpoint diameter for the conusoid was chosen to be 1.5 in. and the midpoint radius 0.75 in. The conical sections forming the end radii are determined by the following two functions: The smaller radius would be the midpoint radius minus half of the midpoint radius, and the larger radius would be the midpoint

radius plus half the midpoint radius. Specimens were fabricated in a mold that was 7 ¾ in. in height. The forward leaning angle, then, is calculated by using the geometry of the specimen and is derived in Equation 1 and illustrated in Figure 2. Note there are infinite combinations of smaller radii, larger radii, and length, resulting in an infinite number of lean angles possible.

$$\theta = \tan^{-1}\left(\frac{r_{large}-r_{small}}{height}\right) = \tan^{-1}\left(\frac{1.125-0.375}{7.75}\right) = 5.5° \qquad (1)$$

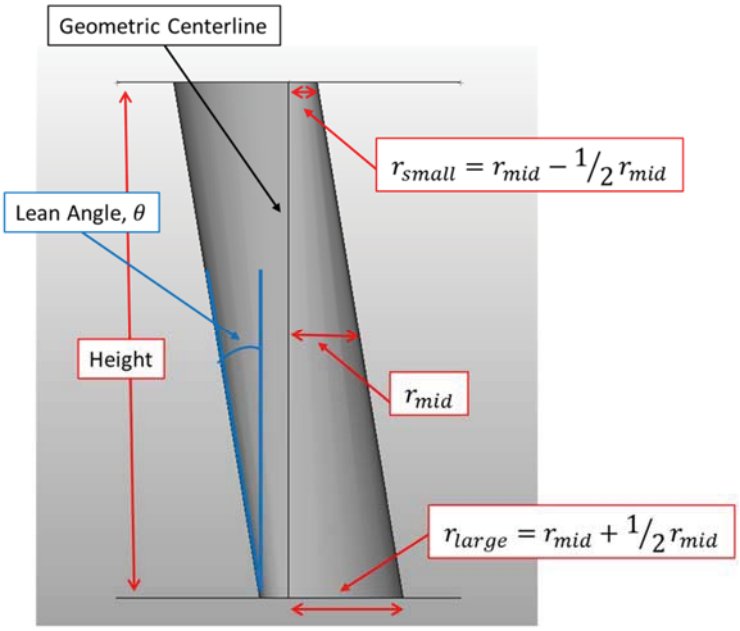

Figure 2. Conusoidal dimensions (side view)

Many potential materials and layup combinations were candidates for the fabrication of the conusoidal EA. Specific interest was given to both the conventional and hybrid families of woven fabrics. Hybrid material systems consisting of carbon and aramid fibers were considered for use since they would potentially contain desirable characteristics that would serve as an advantage for energy absorbing performance. These material systems would offer both stiffness characteristics from the carbon fibers and deformation/ductility characteristics from the aramid fibers. An example of a hybrid woven material is shown in Figure 3, which is an example of carbon/Kevlar plain weave hybrid with the carbon oriented vertically (warp direction) and the Kevlar oriented horizontally (fill direction).

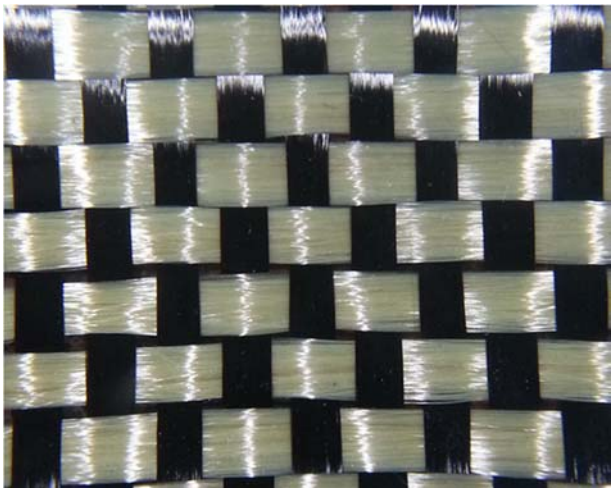

Figure 3. Hybrid carbon / Kevlar plain weave fabric

Additionally, conventional carbon plain, Kevlar plain (K-p) and Kevlar basket (K-b) weaves were also chosen as possible candidates to make pseudo-hybrid material systems. Pseud-hybrid fabrication methods would create laminates with alternating layers of full carbon and full Kevlar weaves to form the layups, potentially offering the same advantages as the woven hybrid materials. Along with the conventional full carbon (c) and full Kevlar (K-p and K-b) material systems, three hybrid systems were chosen for investigation. They were carbon/Kevlar (c/K) plain weave, carbon/Spectra (c/S) twill weave, and carbon/Kevlar twill weave (c/K-t). The entire suite of material systems investigated is summarized in the Table I. Note, when referencing layup directions in this report, the direction angle will always be that of the warp fiber, even though a specific layer may be referred to using the abbreviations above, which are referenced again in Table I.

Table I - Material layups evaluated

Material System #	Type of material	Warp fiber	Fill fiber	Weave	Abbreviation
1	Hybrid	3K Carbon	1140 Kevlar	Plain	c/K
2	Hybrid	3K Carbon	1500 Kevlar	2x2 Twill	c/K-t
3	Hybrid	3K Carbon	Spectra	2x2 Twill	c/S
4	Conventional	3K Carbon	3K Carbon	Plain	c
5	Conventional	Kevlar 49	Kevlar 49	Plain	K-p
6	Conventional	Kevlar 49	Kevlar 49	Basket	K-b

All specimens were wet-laid up using West System 105 epoxy resin with West System 206 hardener, molded within a foam mold, and then placed under vacuum in a vacuum bag for one day to cure at room temperature. Figure 4 shows the

fabrication process. Part A shows the wet layup process of a specimen constructed of a 4 layer c/K material system, Part B shows the layup being placed in the conical mold and Part C shows the conusoidal specimen in the vacuum bag, under vacuum.

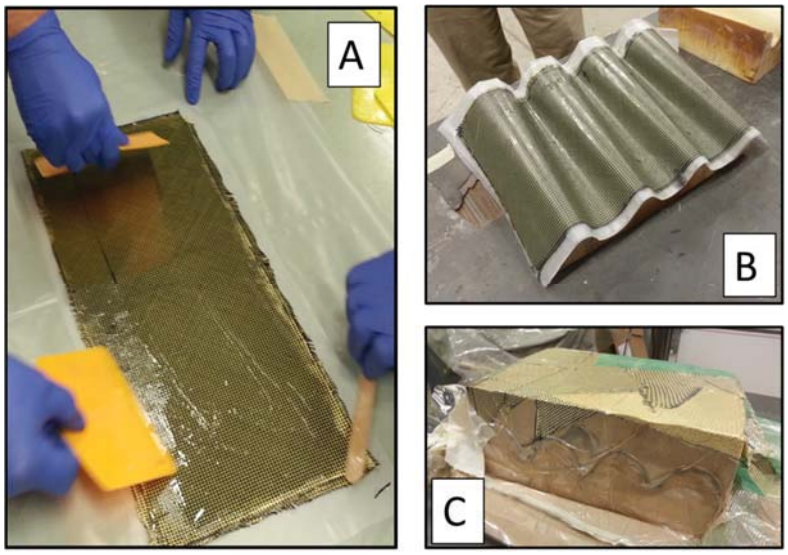

Figure 4. Conusoidal specimen fabrication process

After specimens were removed from the mold, excess edge material was removed and each specimen was ground flat and potted on one end into a half inch polycarbonate plate using West System 105 epoxy resin with West System 206 hardener. The final specimen heights were approximately 7.5 in., and they were approximately 12 in. in length. Volume fraction calculations were completed on a subset of specimens and ranged between 51.5% and 52.3%. Figure 5 shows a completed specimen using the full carbon (c) material system.

Figure 5. Completed conusoidal specimen

MATERIAL TESTING

The material properties were obtained by fabricating specimens containing four layers of each particular material identified in Table I. The conventional woven materials were tested only in the warp direction, with the fill direction assumed to give similar material response. For the hybrid materials, because the fill and warp directions are the primary directions of different materials, tests were conducted in both the warp and fill directions. Tensile tests were conducted in accordance to ASTM 3039 – *Standard Test method for Tensile Properties of Polymer Matrix Composite Materials* [10], and in-plane shear tests were conducted in accordance to ASTM 3518 – *Standard Test method for In-Plane Shear Response of Polymer Matrix Composite Materials by Tensile Test of a ±45° Laminate* [11]. Specimens containing four identical layers were laid up using the techniques described in the previous section; however, the layers were placed on a flat sheet under vacuum and allowed to cure. Final specimen sizes were 1 in. wide by 10 in. long. Specimens were tested in a servo hydraulic test machine at a quasi-static tensile rate of 0.05 in./min. Digital image correlation systems were used to acquire strain in both the specimen axial and lateral directions. An approximate ¼ in. area was chosen at three different points along the gage section and then averaged for use in the stress-strain material response plots. Shear properties were determined from equations used to correlate axial data in the 45 degree direction to shear

response [12]. Figure 6 shows stress-strain responses from the carbon / Kevlar (c/K) hybrid material system.

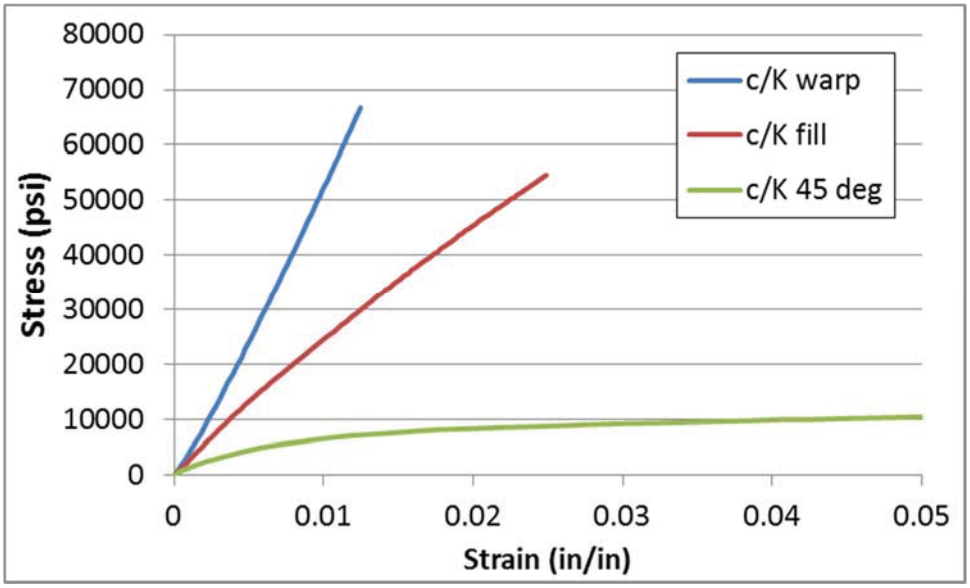

Figure 6. Material response for the carbon / Kevlar material system

The plot shows that the c/K specimens displayed responses consistent with carbon material properties in the warp direction and Kevlar material properties in the fill direction, suggesting that the hybrids were exhibiting a material response that was a combination of both materials. The 45° data extends further outside the range of the plot, however is truncated in order to examine the 0° and 90° directions more clearly. Similar tests were conducted on the other material systems. Table II shows a summary of all of the results for the six material systems tested, noting that the data is an average of two repeat tests.

Table II - Material properties for material systems tested

	Warp Direction			**Fill direction**			**Shear Direction**		
Material System #	**Modulus (psi)**	**Ult. Strength (psi)**	**Ult. Strain (in./in.)**	**Modulus (psi)**	**Ult. Strength (psi)**	**Ult. Strain (in./in.)**	**Modulus (psi)**	**Ult. Strength (psi)**	**Ult. Strain (in./in.)**
1	6.3e6	77.0e3	0.013	2.76e6	54.0e3	0.025	4.5e5	6.1e3	0.45
2*	6.3e6	77.0e3	0.013	2.76e6	54.0e3	0.025	4.5e5	6.1e3	0.45
3	5.4e6	56.0e3	0.011	2.6e6	67.0e3	0.033	3.3e5	8.3e3	0.15
4	6.5e6	76.2e3	0.011	6.5e6	76.2e3	0.011	7.9e5	17.4e3	0.20
5	N/A	N/A	N/A	N/A	N/A	N/A	3.3e5	3.7e3	0.29
6	3.0e6	50.0e3	0.018	3.0e6	50.0e3	0.018	1.0e6	15e3	0.26

**Assumed to be similar to Material System #1*

Material test data show the carbon fiber modulus and strength parameters do not vary significantly when comparing the full carbon woven material and the carbon hybrid woven materials in the warp direction. Figure 7 shows three curves for

specimens which contain the carbon fiber in the warp direction. Note that at low strains (<0.002), while not exactly identical, the material moduli are in good agreement. The ultimate tensile strengths differ; however this can be attributed to specimen-to-specimen variation due to the fabrication process or interactions within the different fill fibers.

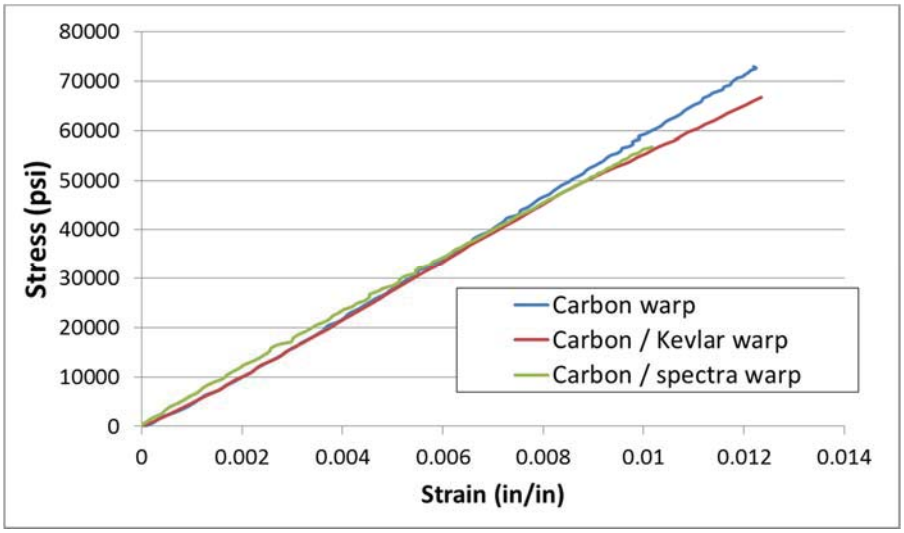

Figure 7. Material system comparison

Material tests were conducted mainly to obtain familiarity with the hybrid and conventional material systems. They were also conducted to determine whether there were any significant deficiencies or reduction factors from the hybrid material systems when compared to the conventional material systems. Note that the specimens used in the impact tests will use combinations of materials layered at various angles and amounts to determine each specimen's specific properties.

IMPACT TESTING OF CONUSOIDAL SPECIMENS

The conusoidal specimens were dynamically crushed in a drop tower with an instrumented 110 lb. falling mass. The impact condition for all of the dynamically crushed specimens was approximately 22 ft./sec. The resultant loading condition gave dynamic crush loads of approximately 100 lbs. per linear foot of specimen at the approximate impact velocity of the TRACT 1 crash test. The 100 lbs. per linear foot loading condition was a conservative assumption based on expected seat and occupant loads that will be introduced to the subfloor during the TRACT 2 impact test. The drop mass was instrumented with a 500 g damped accelerometer and data were acquired using a National Instruments data acquisition system (DAS) sampling at 25 kHz. All post-processed acceleration data was filtered using a low-pass 4-pole Butterworth filter with a 500 Hz cutoff frequency. A high speed camera filming at 1 kHz captured the deformation time history. Video and data

were synchronized using a standard IRIG-B time code system. Figure 8 shows a picture of the test setup.

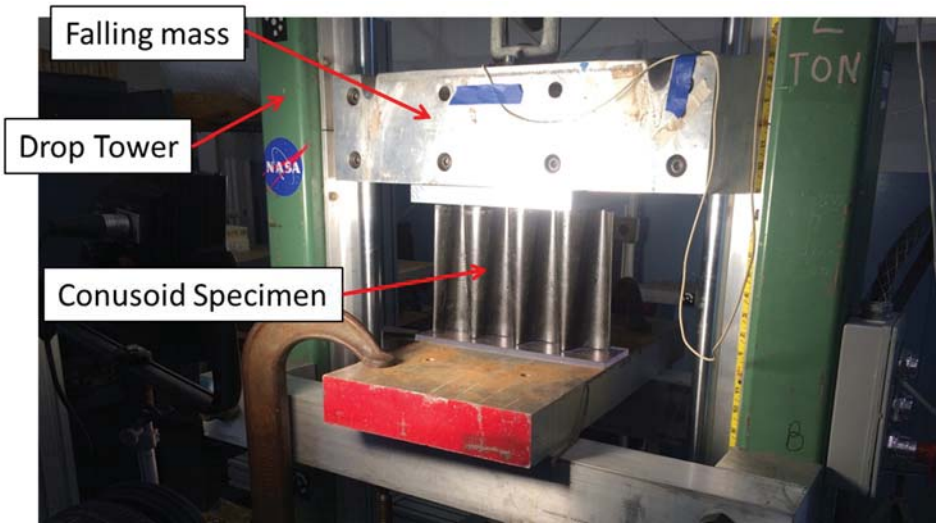

Figure 8. Dynamic test setup

The dynamic testing demonstrated that the specimens failed in mainly three major ways. Figure 9 shows the three failure characteristics as demonstrated from three example specimens. Note that the material and stacking sequence are shown for clarification.

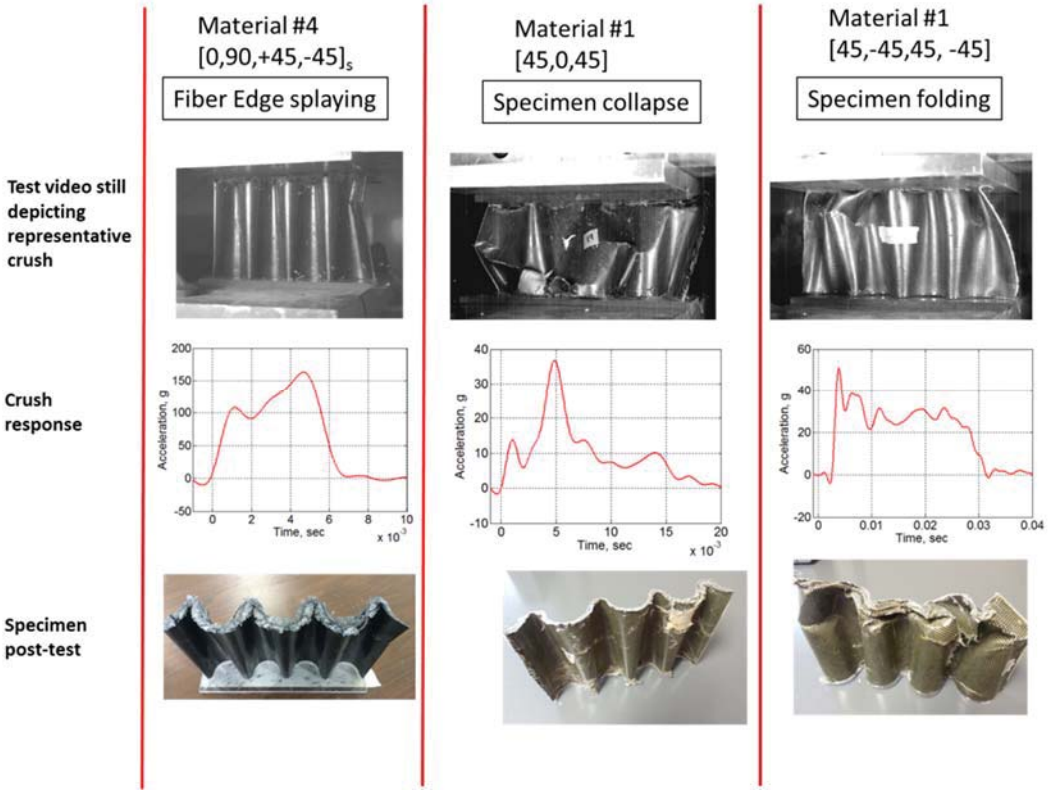

Figure 9. Three major modes of failure in dynamic tests

The fiber edge splaying was evident in a subset of tests, mainly where there was a carbon layer, either hybrid or conventional, with the carbon tows oriented in the 0 degree direction. This is a high energy absorbing mode which, depending on the specific layup, occurs between 50 and 150 g. Figure 9 shows the splaying started at 100 g and ended at approximately 150 g. This type of failure is typical in composite cone crushing [13]. However, the failure mode produced loads at a level too high to be considered for this application, so materials and tests exhibiting this type of behavior were disregarded. The second type of material failure was the complete collapse of the specimen, as demonstrated by the middle column of Figure 9. Typically this type of failure occurred when the specimen walls were too weak and buckled catastrophically. This type of failure usually resulted for specimens having less than 4 layers of material which were simply not stiff enough to sustain a controlled crush. These specimens showed a very low level of attenuation, ranging between 0 and 20 g. The third major type of failure mechanism was the folding of the conusoidal walls. The folding failure was very desirable because it showed a stable and constant crush response at the desired level of between 25 and 40 g, depending on the specific test, material system and layup. A time history is shown in Figure 10 of a specimen folding during the dynamic test.

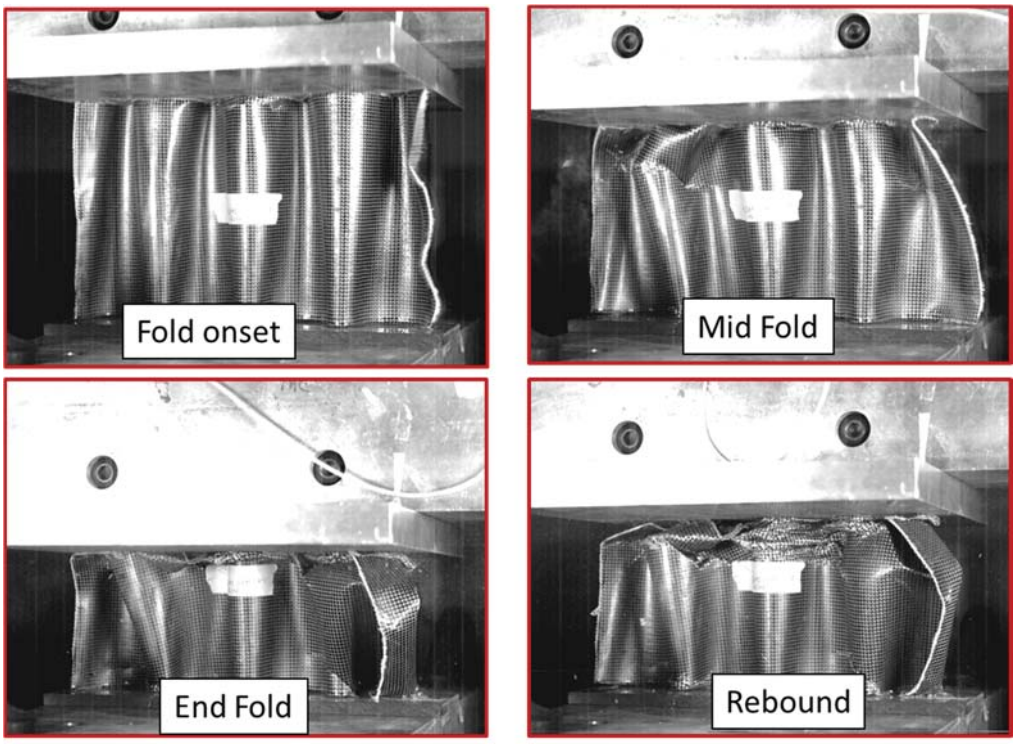

Figure 10. Time history of dynamic test including a fold failure

A total of 24 drop tests were conducted. The folding phenomena only appeared in specimens containing Kevlar or Spectra fibers, and using these materials as a potential screening constraint, the folds only occurred in a small subset of specimens fabricated using different numbers of layers and directions. A few

findings were noted. One major finding was that specimens containing a 0 degree carbon fiber layer did not fold, but rather exhibited an edge splaying failure, as noted above. This finding was proven by comparing [c/k45 c/k-45 c/k-45 c/k45] layup specimen to a [c/k45 c/k0 c/k0 c/k45] layup specimen. Next, specimens that contained more than 4 layers, such as the c/k45 material using 6 and 8 layers, also did not fold, indicating they were much too stiff. Third, specimens having less than three layers collapsed completely under the impact loading, indicating they were too weak. All of these findings were important because they effectively screened the potential material and layup combinations from a large number to a very few. Using the findings presented, the carbon/Kevlar material system in a [c/k45, c/k-45, c/k45, c/k-45] layup was chosen as the final ideal candidate.

Figure 11 shows the close up of the specimen fold in the chosen candidate, and illustrates the cause of the folding phenomena. In a fold, the carbon fiber tows split while the Kevlar fiber tows remained intact, which effectively held the conical wall together. This was a very desirable characteristic expected from the response, and suggested that the carbon can provide the specimen stiffness, while the Kevlar can provide the specimen flexibility.

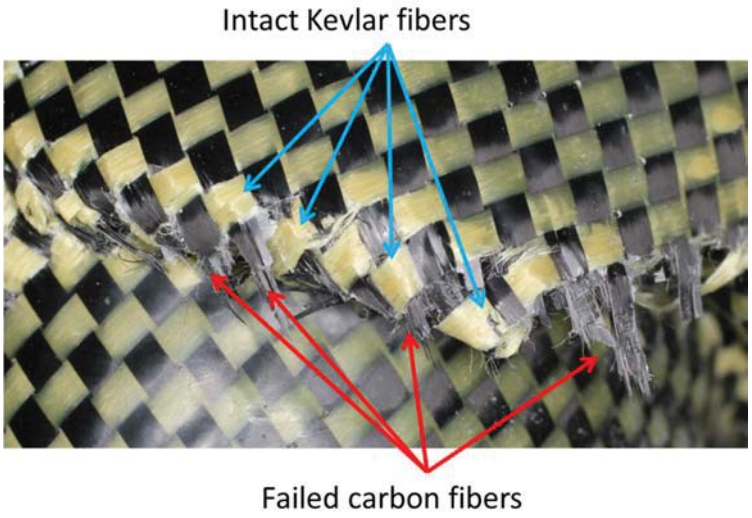

Figure 11. Specimen fold close up

All specimens drop tested in the screening process described above contained a polycarbonate baseplate on one edge and a free edge on the crash front impacted by the falling mass. However, the expected loading in the TRACT 2 test will require the specimens to be fixed at both ends (representing attachment points along both the floor and bottom outer skin). In order to more accurately simulate the expected TRACT 2 boundary conditions, a conusoid specimen was fabricated with two endcaps which more accurately represented the actual attachment conditions, and then drop tested. By testing both a single and a double endcap configuration, the

effect of a potential over-constraint could be analyzed. Figure 12 shows a still frame from the captured high speed video, along with acceleration plots for a test with and without the second endcap.

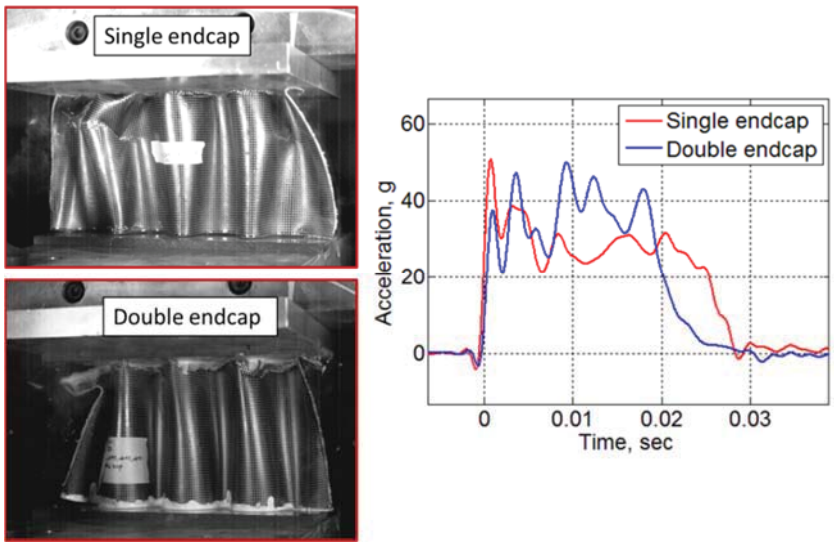

Figure 12. Endcap drop test results

The endcap does make a slight difference in the specimen response as illustrated in Figure 12. Folding still occurred in both the single and double endcap tests. The difference in the response was less than 10 g, and was attributed to the normal scatter in the specimen response, but also potentially from the constraints imposed from the supported sides due to the double endcap condition. One major difference in the response is that the double endcap specimen did not exhibit a noticeable peak crush acceleration, while the one endcap specimen did exhibit a small one. The difference in the crush duration was approximately 5 msec., and the maximum crush stroke for the single endcap was 2.9 in. and the double endcap was 2.5 in. In summary, the double endcap specimen was slightly stiffer than the single endcap specimen due to the additional constraint placed on it by the second endcap. However, the response was still within the realm of potential experimental scatter. The second endcap did not significantly change the behavior of the conusoidal specimen.

STATIC TESTING

Dynamic tests were successful in screening and selecting a potential conusoidal EA design for use in the TRACT 2 crash test. However, to satisfy the second part of the criteria for TRACT 2 implementation, a static test was performed on the selected specimen to ensure it contained enough structural rigidity and static load carrying capability. A [c/k45, c/k-45, c/k45, c/k-45] specimen was fabricated potted into a 2 endcap configuration and placed in a MTS servo-hydraulic test

machine, as shown in Figure 13. The specimen was statically crushed at a rate of 0.1 in./minute until a total crush displacement of 2 in. was achieved. Note that the specimen was painted with a black and white stochastic pattern to allow for the acquisition of photogrammetric strain data.

Figure 13. Static crush specimen

The peak load for the static crush was 5,313 lb., achieved at 0.146 in. of displacement, which is shown in Figure 14. During the post-peak constant crush regime, the static crush load varied between approximately 900 and 1,500 lbs., which was generally constant until 2 in. crush stroke maximum was reached. For the evaluation of CH-46 TRACT 2 test conditions, using the initial slope and peak from the plot, extrapolations can be made. Assuming a 6 ft. span of conusoid which is the approximate span for a frame of the CH-46 which will be used in the TRACT 2 test, a static load of approximately 31,878 lb. can be supported, which is much greater than the expected 900 lb. load arising from 4 ATDs (at approximately 170 lb. a piece) and 2 seats (at 100 lb. a piece). Using a 900 lb. estimate for the expected loading, the static deflection is approximately 0.03 in., which was extracted from the crush load curve in Figure 14.

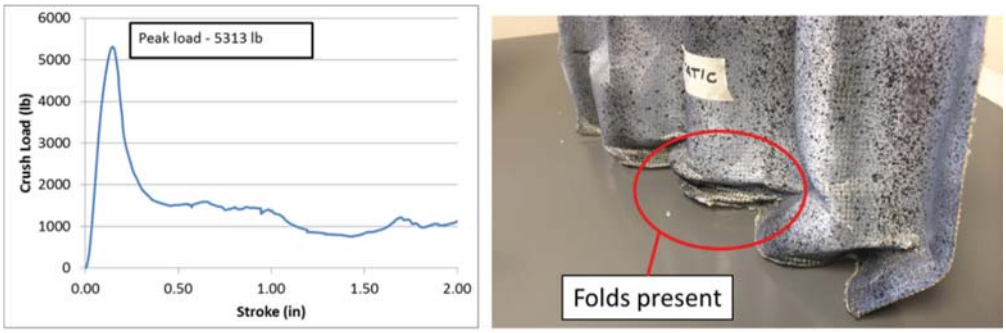

Figure 14. Static crush response and post-test folds

The specimen exhibited the distinct folding crush pattern during quasi-constant post-peak crush loading, which is similar to the response seen in the dynamic crush testing. Much of the variation in the post-peak crush response came from the free sides of the specimen which bent and broke free of the bond due to their unsupported edges. It is expected that on conusoidal specimens having longer spans which contain a larger number of conusoids, the effects from the free edges will be greatly diminished.

SINUSOIDAL COMPARISON

As a final check on the conusoidal geometry, the response of a [c/K45 c/K-45 c/K45 c/K-45] conusoidal specimen was compared to a similar sized sinusoidal specimen. Comparative sinusoidal specimens were fabricated using a keel beam mold of the sine wave design with radii of 0.75 in. One major difference between the sinusoid and the conusoid is that for a 12 in. linear section of beam, the conusoid contained 17.5 in. of material, while the sinusoid contained only 16 in. The extra 1.5 in. was due to the larger changes in radii wrapping around the conical walls, which added an extra 8.5% of material per linear foot. The sinusoid beams were both dynamically and statically tested under identical conditions to the conusoid specimens. The dynamic test results show the conusoid specimen had a lower sustained impact response and more plateau-shaped for a longer response time. This is in contrast to the sinusoid, whose response peaked at approximately 50-g and continually dropped off for the subsequent 20 msec. Note that the initial peak loads for both specimens are the same at approximately 50 g. Figure 15 shows the comparison between the specimens, both in the shape of the response, as shown on the left, and in the acceleration magnitudes, as shown on the right.

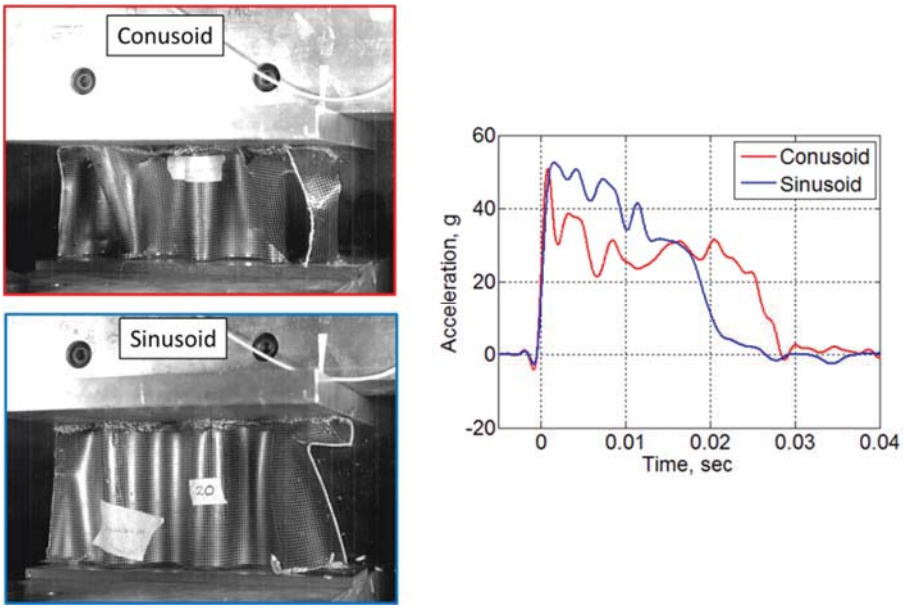

Figure 15. Impact response comparison

A static test was also conducted on a sinusoidal specimen using the same parameters as for the conusoidal specimen. The sinusoidal specimen showed a peak crush load of 4,611 lb., and a sustained crush load of approximately 2,000 lb. Figure 16 shows the comparison between the sinusoid and conusoidal static crush response.

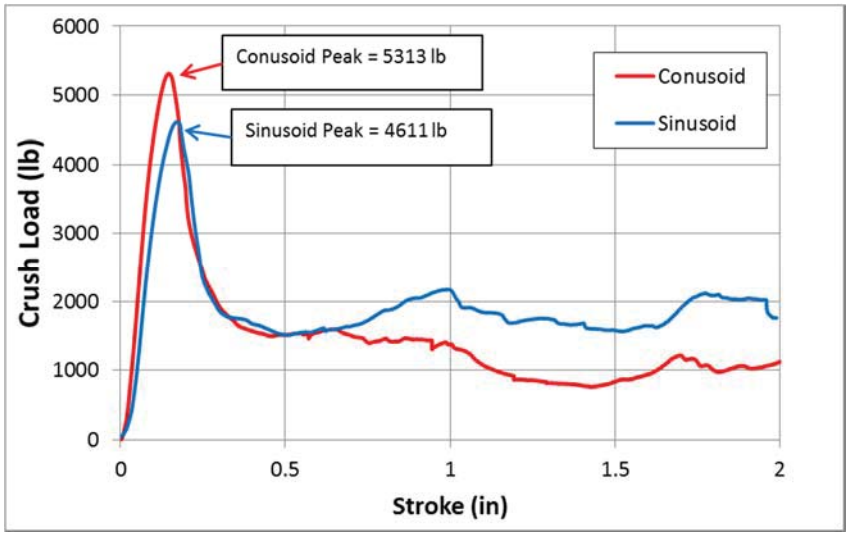

Figure 16. Static crush response comparison

The sinusoid peak crush load was approximately 13% lower than the conusoid. Some of this difference can be attributed to the extra 8.5% of material present in the conusoid or potential manufacturing differences, however, part of the difference could be that the conical geometry is inherently stronger than the sinusoidal geometry. The initial stiffness is also greater with the conusoidal specimen. The

conusoidal specimen reaches the peak load value at 0.143 in. crush displacement, representing a stiffness of 37,153 lb./in., while the sinusoid reaches the peak load at 0.17 in. of displacement, representing a stiffness of 27,123 lb./in. The positions are reversed when examining the post-peak crush response. The sinusoidal specimen is clearly exhibiting a higher post-peak sustained crush response after the 0.5 in. stroke mark. A possible explanation for this phenomenon is that the conusoidal specimen is folding much easier than the sinusoid, likely due to the dissimilar radii present in the conusoid design. The lower post-peak crush load is better because it would limit the load to a lower level than the sinusoidal specimen. In all three benchmarks: the stiffness, the peak load and the post-crush responses, the conusoidal specimen outperformed the sinusoidal specimen. It is initially stiffer, initiates crush at a higher load and crushes at a lower load.

CONCLUSION

The development of a conical energy absorbing specimen, colloquially known as a conusoid, is discussed in the paper. The conical specimen design is developed by placing a simple cone structure in an alternating up-down configuration to make long spans, which look similar to sinusoidal beams. The development of the conusoid includes material selection guidelines, fabric layup conditions, and methods needed in the specimen fabrication.

Once specimens were fabricated, they were screened through dynamic impact testing using an instrumented drop mass. Using information gained from the drop tests, it was determined that the material system of a carbon / Kevlar hybrid fabric laid up in [c/K45 c/K-45 c/K45 c/K-45] configuration achieved the best impact response. This system was further evaluated under static loads, and then compared to a similar sinusoidal specimen. The conusoidal specimen achieved superior performance as compared to the sinusoidal specimen in all parameters examined.

Finally, the data presented confirms that the conusoidal geometry does achieve the required static stiffness and dynamic crush response to be a suitable candidate for inclusion into the TRACT2 full scale crash test. A full scale specimen will be fabricated and retrofitted into the TRACT 2 airframe to evaluate its response in late 2014.

REFERENCES

[1] Annett, M.A. and J.D. Littell. "Evaluation of the Transport Rotorcraft Airframe Crash Testbed (TRACT) Full Scale Crash Test." Proceedings from the FAA Seventh Triennial International Fire & Cabin Safety Conference. December 2-5, 2013.

[2] Price, J.N and D. Hull. "Axial Crushing of Glass Fibre-Polyester Composite Cones." Composites Science and Technology, Vol. 28, 1987.

[3] Feraboli, P. et al. "Design and certification of a composite thin-walled structure for Energy Absorption." International Journal of Vehicle Design, Vol. 44, Nos. 3/4, 2007.

[4] Gupta, N.K. and R. Velmurugan. "Axial Compression of Empty and Foam Filled Composite Conical Shells." Journal of Composite Materials, Vol. 33, No. 6, 1999.

[5] Fleming, D.C and A.J. Vizzini. "Tapered Geometries for Improved Crashworthiness Under Side Loads." Journal of the American Helicopter Society, Vol. 38, 1993.

[6] Farley, G.L and R.M. Jones "Energy Absorption Capability of Composite Tubes and Beams." NASA TM 101634, 1989.

[7] Feraboli, F. "Development of a Corrugated Test Specimen for Composite Materials Energy Absorption." Journal of Composite Materials, Vol. 42, 2008.

[8] Farley, G.L. "A Method of Predicting the Energy-Absorbing Capability of Composite Subfloor Beams." NASA TM 89088. 1987.

[9] Johnson, A.F. et al. "Crash Resistant Composite Subfloor Structures for Helicopters". Proceedings from the AGARD Conference – Advances in Rotorcraft Technology Symposium. AGARD-CP-592. May 27-30, 1996.

[10] American Society for Testing and Materials. "Standard Test Method for Tensile Properties of Polymer Matrix Composite Materials." ASTM-D3039M. 2008.

[11] American Society for Testing and Materials. "Standard Test Method for In-Plane Shear Response of Polymer Matrix Composite Materials by Tensile Test of a ±45° Composite." ASTM-D3518M. 2013.

[12] Lee, S., M. Munro and R.F. Scott. "Evaluation of Three In-Plane Shear Test Methods for Advanced Composite Materials." Composites, Vol. 21, No. 6, 1990.

[13] Morthorst, M. and P. Horst. "Crushing of Conical Composites Shells: A Numerical Analysis of the Governing Factors." Aerospace Science and Technology, Vol. 10, 2006.